Zero : Jurnal Sains, Matematika, dan Terapan
E-ISSN : 2580-5754; P-ISSN : 2580-569X
Volume 9, Number 3, 2025
DOI: 10.30829/zero.v9i3.26488
Page: 991-1003

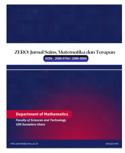

Uncertainty-Aware Kalman Filtering via Intrusive Polynomial Chaos for Disturbance Estimation

[1] **Heri Purnawan**
Department of Electrical Engineering, Universitas Islam Lamongan, Lamongan, Indonesia

[2] **Abdur Rohman Wakhid**
Department of Electrical Engineering, Universitas Islam Lamongan, Lamongan, Indonesia

[3] **Qori' Afiata Fiddina**
Department of Information Technology, Telkom University, Surabaya, Indonesia

[4] **Belgis Ainatul Iza**
Department of Data Science, Universitas Negeri Surabaya, Surabaya, Indonesia

[5] **Tri Muhamad Sanusi**
Department of Electrical Engineering, Universitas Islam Lamongan, Lamongan, Indonesia

[6] **Sari Cahyaningtias**
School of Mathematical and Statistical Sciences, Arizona State University, Arizona, United States

Article Info

Article history:

Accepted 26 December 2025

Keywords:

Disturbance Estimation;
Intrusive Polynomial Chaos;
Kalman Filter;
Measurement Noise;
Parameter Uncertainty.

ABSTRACT

Robust control under parameter uncertainty requires reliable disturbance estimation. This paper proposes an uncertainty-aware method, namely Intrusive Polynomial Chaos-based Kalman Filter (IPC-KF) for systems with probabilistic parameters and measurement noise. The method is evaluated through two numerical case studies and compared with a nominal Kalman filter (KF). Results from 100 realizations, assessed using RMSE and mean variance, show that the IPC-KF achieves estimation accuracy comparable to the nominal KF. For the spring–mass–damper system, the RMSE difference is below 0.01%, with both methods yielding the same mean variance of 0.2133. For the F-16 aircraft model, identical RMSE values and a mean variance of 8.1915×10^{-5} are obtained. While IPC-KF captures parameter uncertainty via polynomial chaos, augmenting the state with disturbances does not necessarily improve estimation accuracy. Further studies are needed to assess uncertainty bounds and robustness.

Corresponding Author:

Heri Purnawan,
Department of Electrical Engineering, Faculty of Science and Technology
Universitas Islam Lamongan,
Email: heripurnawan@unisla.ac.id

1. INTRODUCTION

Disturbances in dynamic systems can significantly degrade control performance if they are not properly addressed during the design stage. In many industrial and aerospace applications—such as flight control in modern aircraft, robotic manipulation, and automotive systems—accurate disturbance estimation plays a crucial role in ensuring robust and stable system behavior [1]. Since disturbances are typically unknown and cannot be measured directly, they are often modeled as extended state variables within the system. Under this assumption—and in the presence of measurement noise—state estimation methods, particularly the Kalman Filter (KF), are widely used to estimate both the system states and disturbances effectively [2], [3].

Another important factor that must be considered in estimation problems is parameter uncertainty. This type of uncertainty arises when the system equations are known, but some parameters are either uncertain or vary over the system's operational lifetime. Such variations frequently occur when models are derived from experimental data using system identification techniques. In these cases, the resulting model is often represented by a transfer function whose parameters vary within certain ranges [4].

These parameter variations introduce significant challenges in designing estimators capable of accurately estimating both system states and disturbances. To achieve robust performance—particularly for disturbance compensation—the estimator must be designed to perform reliably under worst-case conditions. One effective way to address this issue is to represent the uncertain parameters as random variables with known statistical characteristics, such as probability distributions [5]. As modern autonomous, aerospace, and other safety-critical systems increasingly operate in uncertain, noisy, and rapidly varying environments, the need for estimation frameworks that can simultaneously handle probabilistic parameter variations and disturbance dynamics has become more urgent. Conventional deterministic filtering approaches struggle in such conditions, motivating the development of more resilient and uncertainty-aware methods.

Polynomial Chaos Expansion (PCE) provides an efficient framework for representing uncertain parameters and variables as polynomial functions that satisfy orthogonality properties [6], [7]. Compared to Monte Carlo (MC) methods, PCE significantly reduces computational effort while maintaining high accuracy, as demonstrated in various studies [7], [8], [9]. The presence of random parameters in dynamical systems leads to stochastic trajectories, which complicates estimator design. To address this, the stochastic system can be transformed into an equivalent deterministic form using the Intrusive Spectral Projection (ISP) approach [10], [11], [12]. Although the resulting system has higher dimensionality, the ISP method offers high precision for linear systems and facilitates the design of estimation algorithms, since the transformed equations retain a structure similar to the original system.

1.1 Related Work

In previous studies, parameter uncertainty has been addressed either by augmenting uncertain parameters into the state vector [13] or by applying stochastic modeling techniques such as Polynomial Chaos Expansion (PCE) to characterize probabilistic variations [11], [12], [14]. Meanwhile, disturbance handling in control systems has typically relied on Disturbance Observers (DO) and Extended State Observers (ESO), which have proven effective for deterministic disturbance profiles [15], [16], [17], [18]. However, these observer-based approaches are generally not designed to handle probabilistic parameter variations, creating a gap when both effects occur simultaneously. To overcome this limitation, stochastic modeling frameworks—particularly PCE—have been introduced as tools capable of representing uncertainty in a structured manner.

Despite these advances, many existing works treat disturbances and parameter uncertainty separately. Sensor noise is also frequently omitted [15], [16], [17], [19] or, when included, it is only incorporated into the state estimation process without modeling the disturbance itself as a state to be estimated in real time [20], [21], [22], [23], [24], [25]. As a result, prior studies often focus on either uncertainty propagation or state estimation alone, without addressing the combined challenge of estimating disturbances in systems influenced by probabilistic parameter variations and measurement noise.

Collectively, the literature indicates a lack of estimation frameworks that simultaneously model probabilistic parameters, disturbances, and measurement noise within a unified formulation. To further clarify this gap, it is important to highlight the limitations of prior approaches. Most prior studies focused on either parameter uncertainty or disturbance estimation, but not on their combined effects within a single estimation framework, and many PCE-based KF methods primarily address state estimation or uncertainty propagation using non-intrusive or ensemble-based formulations.

In contrast, the present work adopts an intrusive polynomial chaos formulation to derive a deterministic high-dimensional surrogate system in which disturbances are explicitly modeled as extended state variables. This structure enables the direct application of KF with measurement noise, together with explicit observability assumptions on the projected system. These distinctions clarify the novelty of the proposed IPC-KF relative to prior PCE or PC-KF formulations.

1.2 Contribution

The main contributions of this paper are summarized as follows.

- Formulating a stochastic system and its corresponding measurement matrix into a deterministic representation using the ISP approach.
- Developing an implementation of the IPC-KF for estimating disturbances in systems with probabilistic parameters.
- Conducting a comparative analysis with the nominal KF to evaluate the effectiveness and robustness of the proposed method under probabilistic parameters and measurement noise. Throughout this paper, the term nominal KF denotes a Kalman filter constructed using fixed model parameters equal to their mean values, which are kept constant for all realizations in the numerical experiments.

In addition to these contributions, the present study is guided by the following research questions:

- whether incorporating probabilistic parameter information through an intrusive polynomial chaos formulation affects the accuracy and variance of disturbance estimation compared to the nominal KF;
- whether the IPC-KF provides improved robustness or comparable performance under measurement noise and parameter uncertainty; and
- whether modeling disturbances as extended state variables within a stochastic-Galerkin framework offers additional interpretability regarding the impact of parameter uncertainty on estimation performance.

These questions aim to clarify the practical implications and limitations of IPC-KF relative to the nominal KF, rather than to assume inherent performance superiority.

1.3 Structure of This Paper

This paper is organized as follows. Section II presents the design of the proposed IPC-KF method, beginning with the fundamental theory of PCE and followed by the mathematical modeling in terms of the state-space representation and measurement matrix. Section III describes the case studies, which include the Spring–Mass–Damper (SMD) system and the F-16 aircraft model, along with the simulation setup and discussion of the obtained results. Finally, Section IV provides the conclusions and outlines potential directions for future research.

2. RESEARCH METHOD

This research was carried out in two main stages. First, the development stage involved establishing the fundamental theory of PCE, system modeling, and the design of the proposed method. In the second stage, the proposed method was evaluated through numerical case studies, followed by a simulation-based analysis of the results to assess its performance and effectiveness.

2.1 Polynomial Chaos Expansion

The PCE was first introduced by Norbert Wiener to approximate a Gaussian random variable using Hermite polynomials [26]. The core idea behind PCE is to employ an infinite series of orthogonal polynomials. In 1947, the convergence of the Wiener-Hermite polynomial series in the $\mathcal{L}_2$ norm was established in [27].

To facilitate practical implementation, the infinite series of polynomial expansions is truncated as follows [12]:

$$\mathcal{M}(\Delta) = \sum_{n=0}^{N} \tilde{a}_n \, \psi_n(\Delta) \tag{1}$$

In this expression, $\mathcal{M}(\Delta)$ is a random variable defined as a function of the random event Δ, $\tilde{a}_n$ are the polynomial coefficients, and ψ are the polynomial basis functions. The series is truncated after $N+1$ terms, where the number of terms is determined by

$$N + 1 = \frac{\left(n_p + n_\Delta\right)!}{n_p! \; n_\Delta!}$$

with n_p representing the degree of the polynomial and n_Δ is the number of random variables [11].

The choice of polynomial basis in PCE follows the Askey scheme [28], which encompasses a set of orthogonal basis functions in the Hilbert space defined by the support of the random variables. As such, these basis functions satisfy

$$\langle \psi_m(\Delta), \psi_n(\Delta) \rangle = \langle \psi_n^2(\Delta) \rangle \delta_{mn}, \; \delta_{mn} = \begin{cases} 1 & , m = n \\ 0 & , m \neq n \end{cases} \tag{2}$$

where

$$\langle \psi_m(\Delta), \psi_n(\Delta) \rangle = \int_{D_\Delta} \psi_1(\Delta)\psi_2(\Delta) f(\Delta) \; d\Delta = \mathbb{E}[\psi_1(\Delta)\psi_2(\Delta)] \tag{3}$$

denotes the inner product with respect to the weight $f(\Delta)$ (Probability Density Function (PDF) of Δ) and over the domain D_Δ (support of Δ). Using the Galerkin projection method [29], the coefficient $\tilde{a}_n$ is computed by

$$\tilde{a}_n = \frac{\mathbb{E}[M(\Delta)\psi_n(\Delta)]}{\mathbb{E}[\psi_n^2(\Delta)]}$$

The mean and variance of $\mathcal{M}(\Delta)$ can be efficiently approximated from the truncated expansion in Eq. (1) [30]:

$$\mathbb{E}[\mathcal{M}(\Delta)] = \tilde{a}_0 \quad \text{and} \quad \text{Var}[\mathcal{M}(\Delta)] = \sum_{n=1}^{N} \tilde{a}_n^2\, \mathbb{E}[\psi_n^2(\Delta)]$$

2.2 Surrogate Augmented State Space

Consider a discrete-time stochastic linear system characterized by probabilistic time-invariant parameters and unknown disturbances. The system is defined by:

$$\boldsymbol{x}(k+1,\Delta) = \boldsymbol{A}_d(\Delta)\boldsymbol{x}(k,\Delta) + \boldsymbol{B}_d\boldsymbol{d}(k), \tag{4}$$

where $\boldsymbol{x}(k,\Delta) \in \mathbb{R}^p$ is the state vector at time k which is a function of a random variable Δ and $\boldsymbol{d}(k) \in \mathbb{R}^q$ is the unknown disturbance vector at time k, respectively. Here, the state matrix $\boldsymbol{A}_d(\Delta)$ depends on a single random variable Δ, while $\boldsymbol{B}_d$ is the disturbance matrix. Since $\boldsymbol{A}_d$ incorporates randomness, the evolution of the state vector becomes stochastic.

We assume that the disturbance vector remains constant over time and treat it as part of the state vector, the augmented system of Eq. (4) can be rewritten in state space form as:

$$\begin{bmatrix} \boldsymbol{x}(k+1,\Delta) \\ \boldsymbol{d}(k+1) \end{bmatrix} = \begin{bmatrix} \boldsymbol{A}_d(\Delta) & \boldsymbol{B}_d \\ \boldsymbol{0}_{q\times p} & \boldsymbol{I}_p \end{bmatrix} = \begin{bmatrix} \boldsymbol{x}(k,\Delta) \\ \boldsymbol{d}(k) \end{bmatrix} \tag{5}$$

where $\boldsymbol{0}_{q\times p}$ is a zero matrix with size $q \times p$ and $\boldsymbol{I}_q$ is the $q \times q$ identity matrix.

The representation in Eq. (5) allows the system to be expressed as an augmented linear system:

$$\boldsymbol{\phi}(k+1,\Delta) = \boldsymbol{A}(\Delta)\boldsymbol{\phi}(k,\Delta), \tag{6}$$

where $\boldsymbol{\phi} = [\boldsymbol{x}^T, \boldsymbol{d}^T]^T \in \mathbb{R}^{p+q}$ is the augmented state vector and $\boldsymbol{A}(\Delta)$ represents the new state matrix of the augmented system. Since $\boldsymbol{A}(\Delta)$ depends on random variables, the evolution of the augmented state vector in Eq. (6) remains stochastic, similar to the original system in Eq. (4).

Theorem 2.2. The surrogate augmented state space representation of system in Eq. (6) obtained using the IPC approach can be written as the deterministic system

$$\boldsymbol{\Phi}(k+1) = \boldsymbol{\mathcal{A}}\boldsymbol{\Phi}(k) \tag{7}$$

where state vector is defined as $\boldsymbol{\Phi} = \left[\widetilde{\boldsymbol{\phi}}_1^T, \ldots, \widetilde{\boldsymbol{\phi}}_{p+q}^T\right]^T \in \mathbb{R}^{(p+q)(N+1)}$, and each block

$$\widetilde{\boldsymbol{\phi}}_i(k) = \left[\tilde{\phi}_{i,0}(k), \ldots, \tilde{\phi}_{i,N}(k)\right]^T, \quad i = 1, \ldots, p+q.$$

The system matrix $\boldsymbol{\mathcal{A}} \in \mathbb{R}^{(p+q)(N+1)\times(p+q)(N+1)}$ is given by

$$\boldsymbol{\mathcal{A}} = \begin{bmatrix} \mathcal{A}_{11} & \cdots & \mathcal{A}_{1(p+q)} \\ \vdots & \ddots & \vdots \\ \mathcal{A}_{(p+q)1} & \cdots & \mathcal{A}_{(p+q)(p+q)} \end{bmatrix}$$

where each block $\mathcal{A}_{ij} \in \mathbb{R}^{(N+1)\times(N+1)}$ is given by

$$\mathcal{A}_{ij} = \sum_{n=0}^{N} \tilde{A}_{ij,n}\, \boldsymbol{\varphi}_n,$$

where

$$\boldsymbol{\varphi}_n = \begin{bmatrix} \gamma_{n00} & \cdots & \gamma_{nN0} \\ \vdots & \ddots & \vdots \\ \gamma_{n0N} & \cdots & \gamma_{nNN} \end{bmatrix}.$$

Proof. Assume that $\boldsymbol{\phi}(k,\Delta), \boldsymbol{A}(\Delta) \in \mathcal{L}_2$, so that all expectations used in the projection are finite. The random variable Δ is assumed to follow a distribution matched to the corresponding Askey polynomial basis $\{\psi_n(\Delta)\}_{n=1}^N$ which satisfies the orthogonality property in Eq. (2). We further assume that $\boldsymbol{A}(\Delta)$ is Lipschitz-continuous in Δ, and that Δ has either bounded support or sub-Gaussian tails. These assumptions guarantee integrability and justify the interchange of expectation, multiplication, and the discrete-time update operator in the projection steps that follow.

The construction of the augmented state space via an intrusive approach based on PCE can be outlined by defining each augmented state $\phi_i \in \boldsymbol{\phi}$ and state matrix $A_{ij} \in \boldsymbol{A}$, using Eq. (1) as follows.

$$\phi_i(k,\Delta) = \sum_{n=0}^{N} \tilde{\phi}_n(k)\psi_n(\Delta) \tag{8}$$

$$A_{ij}(\Delta) = \sum_{n=0}^{N} \tilde{A}_{ij,n}\,\psi_n(\Delta) \tag{9}$$

Substitute Eqs. (8) and (9) into Eq. (6) to obtain

$$\sum_{l=0}^{N} \tilde{\phi}_{i,l}(k+1)\psi_l(\Delta) = \sum_{j=1}^{p+q}\sum_{l=0}^{N}\sum_{m=0}^{N} \tilde{A}_{ij,l}\,\tilde{\phi}_{j,m}(k)\psi_l(\Delta)\psi_m(\Delta) \tag{10}$$

Multiply both side by $\psi_n(\Delta), n = 0,\cdots,N,$ and take the expectation with Δ, Eq. (10) can be simplified to

$$\sum_{l=0}^{N} \tilde{\phi}_{i,l}(k+1)\mathbb{E}[\psi_l(\Delta)\psi_n(\Delta)] = \sum_{j=1}^{p+q}\sum_{l=0}^{N}\sum_{m=0}^{N} \tilde{A}_{ij,l}\,\tilde{\phi}_{j,m}(k)\mathbb{E}[\psi_l(\Delta)\psi_m(\Delta)\psi_n(\Delta)]$$

For readability, we omit the explicit dependence on Δ in the basis functions, i.e. $\psi_n(\Delta)$ is written simply as ψ_n. Using the orthogonality property in Eq. (2), $\mathbb{E}[\psi_l(\Delta)\psi_n(\Delta)] = \mathbb{E}[\psi_n^2]$ and defining the triple-product tensor $\mathbb{E}[\psi_l(\Delta)\psi_m(\Delta)\psi_n(\Delta)] = \mathbb{E}[\psi_l\psi_m\psi_n]$, we have

$$\tilde{\phi}_{i,n}(k+1)\mathbb{E}[\psi_n^2] = \sum_{j=1}^{p+q}\sum_{l=0}^{N}\sum_{m=0}^{N} \tilde{A}_{ij,l}\,\tilde{\phi}_{j,m}(k)\mathbb{E}[\psi_l\psi_m\psi_n] \tag{11}$$

Divide Eq. (11) by $\mathbb{E}[\psi_n^2]$ to yield

$$\begin{aligned}\tilde{\phi}_{i,n}(k+1) &= \frac{1}{\mathbb{E}[\psi_n^2]}\sum_{j=1}^{p+q}\sum_{l=0}^{N}\sum_{m=0}^{N} \tilde{A}_{ij,l}\,\tilde{\phi}_{j,m}(k)\mathbb{E}[\psi_l\psi_m\psi_n] \\ &= \sum_{j=1}^{p+q}\sum_{l=0}^{N}\sum_{m=0}^{N} \tilde{A}_{ij,l}\,\tilde{\phi}_{j,m}(k)\,\gamma_{lmn}\end{aligned} \tag{12}$$

In the intrusive polynomial chaos framework, the products of polynomial expansions lead to triple products of basis functions. These interactions are compactly represented by the triple-product coefficients, where $\gamma_{lnm} = \mathbb{E}[\psi_l\psi_m\psi_n]/\mathbb{E}[\psi_n^2]$. For $m = 0, 1, \cdots, N$, Eq. (12) can be written as:

$$\tilde{\phi}_{i,n}(k+1) = \sum_{j=1}^{p+q}\sum_{l=0}^{N} \tilde{A}_{ij,l}[\gamma_{l0n} \quad \gamma_{l1n} \quad \cdots \quad \gamma_{lNn}]\begin{bmatrix}\tilde{\phi}_{j,0}(k)\\ \tilde{\phi}_{j,1}(k)\\ \vdots \\ \tilde{\phi}_{j,N}(k)\end{bmatrix}$$

Define $\tilde{\boldsymbol{\phi}}_i(k) = \left[\tilde{\phi}_{i,0}(k), \dots, \tilde{\phi}_{i,N}(k)\right]^T, i = 1, \dots, p+q$, we obtain

$$\tilde{\boldsymbol{\phi}}_i(k+1) = \sum_{j=1}^{p+q}\sum_{l=0}^{N} \tilde{A}_{ij,l}\begin{bmatrix}\gamma_{l00} & \cdots & \gamma_{lN0}\\ \vdots & \ddots & \vdots \\ \gamma_{l0N} & \cdots & \gamma_{lNN}\end{bmatrix}\tilde{\boldsymbol{\phi}}_j(k) = \sum_{j=1}^{p+q}\sum_{l=0}^{N} \tilde{A}_{ij,l}\,\boldsymbol{\varphi}_l\tilde{\boldsymbol{\phi}}_j(k) \tag{13}$$

where

$$\boldsymbol{\varphi}_l = \begin{bmatrix}\gamma_{l00} & \cdots & \gamma_{lN0}\\ \vdots & \ddots & \vdots \\ \gamma_{l0N} & \cdots & \gamma_{lNN}\end{bmatrix}.$$

To obtain a compact deterministic state-space representation, the polynomial-mode coupling coefficients are assembled into a vector. Let $\boldsymbol{\Phi} = \left[\tilde{\boldsymbol{\phi}}_1^T, \dots, \tilde{\boldsymbol{\phi}}_{p+q}^T\right]^T$, then Eq. (13) becomes the deterministic state-space equation

$$\boldsymbol{\Phi}(k+1) = \boldsymbol{\mathcal{A}}\boldsymbol{\Phi}(k),$$

where

$$\boldsymbol{\mathcal{A}} = \begin{bmatrix}\mathcal{A}_{11} & \cdots & \mathcal{A}_{1(p+q)}\\ \vdots & \ddots & \vdots \\ \mathcal{A}_{(p+q)1} & \cdots & \mathcal{A}_{(p+q)(p+q)}\end{bmatrix}$$

with

$$\mathcal{A}_{ij} = \sum_{l=0}^{N} \tilde{A}_{ij,l}\, \boldsymbol{\varphi}_l, \forall i,j = 1,2,\cdots,(p+q)$$

Under the stated regularity assumptions, all projection operations above are valid, and the deterministic surrogate model follows directly. Therefore, the proof is complete.

2.3 Measurement Matrix

The use of an ISP approach to propagate the uncertainty Δ transforms the system into a higher-dimensional deterministic form, represented by the surrogate state vector $\boldsymbol{\Phi}$, which contains the PCE coefficients. Consequently, the measurement model must be adapted to align with this surrogate state representation.

Assumption 2.4. For the theoretical derivation and estimator design, the process dynamics are assumed to be noise-free, i.e., $\boldsymbol{w}(k) = \boldsymbol{0}$. This assumption is used exclusively in all projection arguments and proofs presented in this section. However, the measurement data are considered to be corrupted by additive Gaussian white noise with zero mean and covariance $\boldsymbol{R}$, denoted as $\boldsymbol{v}(k) \sim \mathcal{N}(0,\boldsymbol{R})$.

In practice, a small process noise is introduced only for numerical stability of the KF and IPC-KF, and does not alter the theoretical formulation derived under **Assumption 2.4**.

Theorem 2.5. The discrete-time measurement model due to probabilistic parameters is given as follows.

$$\boldsymbol{z}(k,\Delta) = \boldsymbol{C}\boldsymbol{\phi}(k,\Delta), \tag{14}$$

where $\boldsymbol{z} \in \mathbb{R}^p$ is the measurement vector and $\boldsymbol{C}$ is the measurement matrix under disturbance measurement not available. Due to the surrogate state representation $\boldsymbol{\Phi}(k)$ of the intrusive PCE method, the measurement equation becomes

$$\boldsymbol{Z}(k) = \boldsymbol{\mathcal{C}}\boldsymbol{\Phi}(k), \tag{15}$$

where $\boldsymbol{Z} = \left[\tilde{\boldsymbol{z}}_1^{\top},\ldots,\tilde{\boldsymbol{z}}_p^{\top}\right]^{\top} \in \mathbb{R}^{(p+q)(N+1)}$, with each block defined by $\tilde{\boldsymbol{z}}_i(k) = [\tilde{z}_{i,0},(k),\ldots,\tilde{z}_{i,N}(k)]^T, \forall i = 1,\ldots,p$ and $\boldsymbol{\mathcal{C}} = \boldsymbol{C} \otimes \boldsymbol{I}_{N+1}$ with $\boldsymbol{I}_{N+1}$ is the identity matrix.

Proof. Define $c_{ij} \in \boldsymbol{C}$ and implement each state variable in PCE term given in Eq. (8) as well as a measurement variable while ignoring Δ for simplification, for $\boldsymbol{i} = 1,\cdots,p$ we obtain

$$\sum_{m=0}^{N} \tilde{z}_{i,m}(k)\psi_m = \sum_{j=1}^{p+q} c_{ij} \sum_{m=0}^{N} \tilde{\Phi}_{j,m}(k)\psi_m \tag{16}$$

Multiply both sides of Eq. (16) with $\{\psi_n\}_{n=0}^{N}$ and take the expectation, to yield

$$\sum_{m=0}^{N} \tilde{z}_{i,m}(k)\mathbb{E}[\psi_m\psi_n] = \sum_{j=1}^{p+q} \sum_{m=0}^{N} c_{ij}\tilde{\Phi}_{j,m}(k)\mathbb{E}[\psi_m\psi_n]$$

Then apply orthogonal property to obtain

$$\tilde{z}_{i,n}(k)\mathbb{E}[\psi_n^2] = \sum_{j=1}^{p+q} \sum_{m=0}^{N} c_{ij}\tilde{\Phi}_{j,m}(k)\mathbb{E}[\psi_n^2] \tag{17}$$

Divide Eq. (17) by $\mathbb{E}[\psi_n^2]$, we simplify Eq. (16) to

$$\tilde{z}_{i,n}(k) = \sum_{j=1}^{p+q} \sum_{m=0}^{N} c_{ij}\tilde{\Phi}_{j,m}(k) \tag{18}$$

Since Eq. (18) is equivalent to Eq. (15), this completes the proof.

Remark 2.6. The measurement variable must be extended in terms of the PCE coefficients. If the measurement dimension were kept identical to that of the original system, the resulting surrogate system would not satisfy the observability condition. Consequently, the disturbance estimate would not be guaranteed to converge to the true disturbance.

2.4 Intrusive Polynomial Chaos-based Kalman Filter

The IPC-KF is introduced to estimate disturbances under probabilistic system parameters. Its design is based on the surrogate dynamic system. To enable the estimation of disturbances modeled as state vectors, the observability condition in this framework is ensured by **Lemma 2.7**.

Lemma 2.7. (Sufficient Observability Condition) Suppose the parameter-dependent pair $(\boldsymbol{A}(\Delta), \boldsymbol{C})$ is uniformly observable for all Δ in the support of the random parameter. Then the surrogate pair $(\boldsymbol{\mathcal{A}}, \boldsymbol{\mathcal{C}})$ obtained from Eqs. (7) and (15) is observable for any truncation order N, provided the triple-product tensor constructed from the basis has full row rank.

Lemma 2.7 is motivated by the fact that observability of the nominal dynamics, associated with the constant polynomial chaos mode, is preserved under the Galerkin projection. The coupling induced by the triple-product tensor transfers this observability to higher-order modes, provided the tensor has full row rank, yielding observability of the augmented surrogate system.

Assumption 2.8. Consider the discrete-time surrogate system in Eqs. (7) and (14). The system is assumed to be observable, with the observability matrix defined as

$$\mathcal{O} = [\boldsymbol{\mathcal{C}}, \boldsymbol{\mathcal{C}\mathcal{A}}, \boldsymbol{\mathcal{C}\mathcal{A}}^2 \ \dots \ \boldsymbol{\mathcal{C}\mathcal{A}}^{(p+q)(N+1)-1}]^{\mathrm{T}}.$$

This implies that the rank of the observability matrix is

$$\mathrm{rank}(\mathcal{O}) = (p+q)(N+1).$$

The IPC-KF algorithm is built in a way similar to the nominal KF, but it operates in a higher-dimensional space than the original system. Prior to running the IPC-KF, the polynomial degree n_p is selected based on surrogate convergence tests. The process noise covariance is set to $\boldsymbol{Q} > 0$ for numerical robustness, while the measurement noise covariance $\boldsymbol{R}$ is determined from empirical sensor noise statistics. The initial PCE coefficient vector $\widehat{\boldsymbol{\Phi}}(0|0) = \boldsymbol{\phi}(0) \otimes \boldsymbol{e}_{N+1}$, $\boldsymbol{e}_{N+1} = \underbrace{[1 \ 0 \ \cdots \ 0]}_{N+1}$ and the initial covariance $\mathbf{P}(0|0) = \mathrm{diag}\,\underbrace{(10^{-1}, \cdots, 10^{-1})}_{p+q} \otimes \boldsymbol{I}_{N+1}$ is chosen as a diagonal matrix encoding prior uncertainty. The IPC-KF procedure, which is derived from the surrogate system, can be summarized in **Algorithm 1**.

Algorithm 1 IPC-KF for disturbance estimation

Input: Measurement $z_i(k), i = 1, \dots, p$ and $k = 0, \dots, N_{\mathrm{iter}}$, degree of polynomial n_p, noise covariance matrices $\boldsymbol{Q}$ and $\boldsymbol{R}$, initial condition $\boldsymbol{\phi}(0)$, sampling time T_s, and time duration for simulation t_f.

1. Define PDFs of uncertain parameters Δ.
2. Form augmented state including disturbance
3. Construct PCE basis ψ and expand system matrices $(\boldsymbol{A}(\Delta), \boldsymbol{C})$.
4. Apply Galerkin projection to obtain surrogate system $(\boldsymbol{\mathcal{A}}, \boldsymbol{\mathcal{C}})$.
5. Initialization:

    $\widehat{\boldsymbol{\Phi}}(0|0) = \widehat{\boldsymbol{\Phi}}_0$
    $\mathbf{P}(0|0) = \mathbf{P}_0$

Set $k \leftarrow 0$

for $k \leftarrow 1 : N_{iter} = \frac{t_f}{T_s}$ **do**

  Time update:

    $\widehat{\boldsymbol{\Phi}}(k|k-1) = \boldsymbol{\mathcal{A}}\widehat{\boldsymbol{\Phi}}\,(k-1|k-1)$
    $\mathbf{P}(k|k-1) = \boldsymbol{\mathcal{A}}\mathbf{P}(k-1|k-1)\boldsymbol{\mathcal{A}}^{\mathrm{T}} + \overline{\mathbf{Q}}$

  Measurement update:

    $\mathbf{K}(k) = \mathbf{P}(k|k-1)\boldsymbol{\mathcal{C}}^{\mathrm{T}}(\boldsymbol{\mathcal{C}}\mathbf{P}(k|k-1)\boldsymbol{\mathcal{C}}^{\mathrm{T}} + \overline{\mathbf{R}})^{-1}$
    $\widehat{\boldsymbol{\Phi}}(k|k) = \widehat{\boldsymbol{\Phi}}(k|k-1) + \mathbf{K}(k)\left(\boldsymbol{Z}(k) - \boldsymbol{\mathcal{C}}\widehat{\boldsymbol{\Phi}}(k|k-1)\right)$
    $\mathbf{P}(k|k) = \left(\boldsymbol{I}_{(p+q)(N+1)} - \mathbf{K}(k)\boldsymbol{\mathcal{C}}\right)\mathbf{P}(k|k-1)$

end

Result: $\hat{\hat{\phi}}_{i,n}(k|k), \quad i = (p+1), \dots, (p+q)$

Remark 2.9. Even though noise-free for the process dynamics according to **Assumption 2.4**, the noise covariance matrix is defined by $\overline{\mathbf{Q}} = \boldsymbol{Q} \otimes \boldsymbol{I}_{N+1}$. In practical implementations, a small process-noise covariance $\boldsymbol{Q} > \mathbf{0}$ may be introduced for numerical stability of the discrete-time estimator, but this does not affect the analytical results or the polynomial chaos projection. The initial state covariance is chosen to be diagonal, reflecting an uninformative prior assumption with no prescribed cross-correlation among the augmented states.

To evaluate the capability of the IPC-KF method in estimating disturbances, we consider N_Δ realizations of the parameters where each realization produces $N_{\text{iter}} + 1$ measurement sequences.

3. RESULT AND ANALYSIS

To evaluate the performance of the IPC-KF in propagating probabilistic parameters and estimating disturbances, two representative case studies are presented: SMD and F-16 aircraft systems. These examples are selected to demonstrate the applicability of the proposed approach to both a simple mechanical model and a more complex aerospace system. The simulation scenario is considered using zero initial condition $\boldsymbol{\phi}(0) = [0,0,0]^\mathrm{T}$. The noise covariance matrix is defined $\bar{\mathbf{R}} = \boldsymbol{R} \otimes \boldsymbol{I}_{N+1}$ where $\boldsymbol{R} = \text{diag}\ \underbrace{(10^{-4}, \cdots, 10^{-4})}_{p}$. In this study, the uncertain parameter Δ is modeled as a uniformly distributed random variable. The uniform distribution serves as a non-informative and bounded prior, which is commonly used when no specific probabilistic profile of the parameter is assumed.

3.1 Example 1: Spring-Mass-Damper

The SMD system, characterized by an uncertain spring stiffness coefficient k_s and driven by a disturbance d, is described by

$$m\ddot{x}(t) + c\dot{x}(t) + k_s x(t) = d(t) \tag{19}$$

The mass of the system is fixed at $m = 1$ and is released from the initial position $x(0) = 5$ with zero initial velocity, $\dot{x}(0) = 0$. The simulation is carried out over the interval $t \in [0, t_f]$, where t_f denotes the final time. The damping constant is known and set to $c = 0.1$. The state evolution of the nominal system, corresponding to $k_s = 2$ in the absence of external disturbance $d(t) = 0$, is illustrated in **Figure 1**.

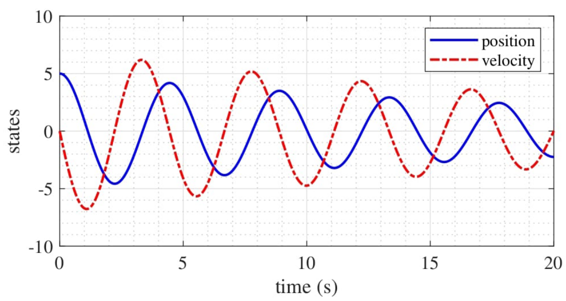

Figure 1. The state evolution of nominal parameter $(k_s = 2)$

The spring stiffness k_s is assumed to follow a uniform distribution, $k_s \sim \mathcal{U}(1.5, 2.5)$, while the external force as disturbance is represented by $d(t)$. For ease of simulation, Eq. (18) is expressed in state-space form as

$$\begin{bmatrix} \dot{x}_1 \\ \dot{x}_2 \end{bmatrix} = \begin{bmatrix} 0 & 1 \\ -k_s & -0.1 \end{bmatrix} \begin{bmatrix} x_1 \\ x_2 \end{bmatrix} + \begin{bmatrix} 0 \\ 1 \end{bmatrix} d \tag{20}$$

where x_1 and x_2 denote the position and velocity states, respectively. The spring stiffness k_s is subject to 25% deviation around its nominal value and is modeled as

$$k_s = 2 + 0.5\Delta, \Delta \sim \mathcal{U}(-1,1)$$

To implement the IPC-KF algorithm, the continuous-time model in Eq. (20) is discretized using the Euler method with a sampling period $\Delta t = 0.01$ s, yielding

$$\begin{bmatrix} x_1(k+1) \\ x_2(k+1) \end{bmatrix} = \begin{bmatrix} 1 & 0.01 \\ -0{,}01k_s & 0.999 \end{bmatrix} \begin{bmatrix} x_1(k) \\ x_2(k) \end{bmatrix} + \begin{bmatrix} 0 \\ 0.01 \end{bmatrix} d(k) \tag{21}$$

where the discrete index k is defined as $k = t/\Delta t$.
Transforming Eq. (21) into the augmented state-space form Eq. (6) in discrete time, we define

$$\phi = \begin{bmatrix} x_1 \\ x_2 \\ d \end{bmatrix}, \text{and } \boldsymbol{A}(\Delta) = \begin{bmatrix} 1 & 0.01 & 0 \\ -0.01k_s & 0.999 & 0.01 \\ 0 & 0 & 1 \end{bmatrix}$$

Assuming that only the states of the SMD system are measurable, the measurement matrix is given by

$$\boldsymbol{C} = \begin{bmatrix} 1 & 0 & 0 \\ 0 & 1 & 0 \end{bmatrix}$$

The polynomial degree is set to $n_p = 2$, which leads to $N + 1 = (2 + 1)!/2!\,1! = 3$ terms in the polynomial expansion The disturbance is modeled as a constant signal, $d(k) = 2$. The results of these scenarios are shown in **Figure 2**.

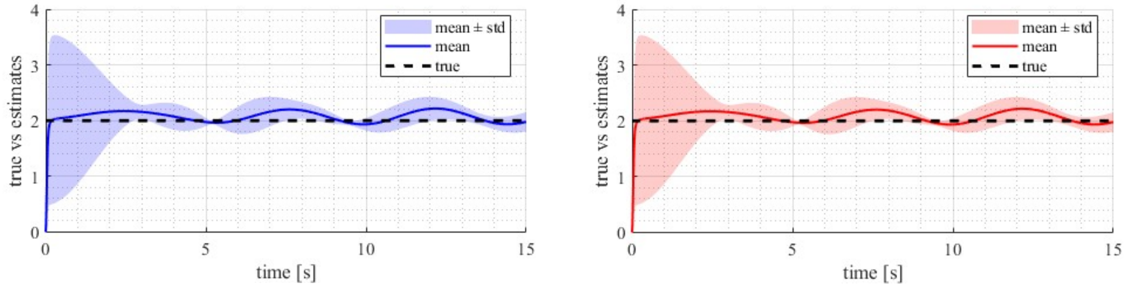

(a) Nominal KF ($\boldsymbol{R} = 10^{-4}\boldsymbol{I}_2$) (b) IPC-KF

Figure 2. Comparison of disturbance estimations for SMD system with 100 random variables, Δ.

Figures 2(a) and **(b)** present the results of the nominal KF (with $\Delta = 0$ for all realizations) and the IPC-KF method, respectively. From these figures, it can be observed that both methods are able to track the true disturbance despite the presence of parameter uncertainty and measurement noise. Although the estimations do not perfectly match the true disturbance, the results for each realization remain close to the actual value. Furthermore, the shaded area becomes narrower, indicating reduced estimation variability and convergence toward the true disturbance.

3.2 Example 2: F-16 aircraft

The F-16 is a fighter aircraft whose nonlinear aerodynamic characteristics make it difficult to obtain an exact mathematical model of its dynamics. This challenge primarily arises at high angles of attack, where aerodynamic coefficient modeling becomes inaccurate. The state-space equation for the short-period mode in discrete time, discretized from [31] using the Euler method with the same sampling time as in Example 1, and under time-invariant probabilistic parameters, is given by

$$\begin{bmatrix} \alpha(k+1) \\ q(k+1) \\ x_E(k+1) \end{bmatrix} = \begin{bmatrix} 0.9936 & 0.0094 & -1.4\times 10^{-5} \\ a_{21}(\Delta) & a_{22}(\Delta) & a_{23}(\Delta) \\ 0 & 0 & 0.7980 \end{bmatrix} \begin{bmatrix} \alpha(k) \\ q(k) \\ x_E(k) \end{bmatrix} + \begin{bmatrix} 0 \\ 0 \\ 0.202 \end{bmatrix} d(k). \tag{22}$$

Here, α denotes the angle of attack, q is the pitch rate, and x_E represents the elevator state, which captures actuator dynamics. The parameters are assumed to follow a uniform distribution with a deviation of 20% from their nominal values, defined as

$$a_{21}(\Delta) = -0.0157(1 + 0.2\Delta),$$
$$a_{22}(\Delta) = 0.9912(1 + 0.2\Delta),$$
$$a_{23}(\Delta) = -0.0011(1 + 0.2\Delta).$$

where the randomness of these parameters is governed by a single random variable $\Delta \sim \mathcal{U}(-1,1)$.

By augmenting the system to include the disturbance as an additional state variable, the discrete-time state-space representation becomes

$$\boldsymbol{\phi}(k+1) = \boldsymbol{A}(\Delta)\boldsymbol{\phi}(k) \tag{23}$$

where $\boldsymbol{\phi} = [\alpha, q, x_E, d]^{\mathrm{T}}$ and $\boldsymbol{A}(\Delta)$ is given by

$$\boldsymbol{A}(\Delta) = \begin{bmatrix} 0.9936 & 0.0094 & -1.4\times 10^{-5} & 0 \\ a_{21}(\Delta) & a_{22}(\Delta) & a_{23}(\Delta) & 0 \\ 0 & 0 & 0.7980 & 0.202 \\ 0 & 0 & 0 & 1 \end{bmatrix}$$

Since the disturbance is unknown and unmeasurable, the measurement matrix for this case is defined as

$$\boldsymbol{C} = \begin{bmatrix} 1 & 0 & 0 & 0 \\ 0 & 1 & 0 & 0 \\ 0 & 0 & 1 & 0 \end{bmatrix}$$

The parameter settings in this simulation are set different from Example 1, particularly for adding noise covariance matrices for $\boldsymbol{Q}$ and $\bar{\mathbf{Q}}$. This configuration is introduced to prevent divergence in the disturbance estimation, since the system derived from the ISP approach exhibits an eigenvalue exceeding one, which signifies that the system is unstable. The disturbance is modeled as a constant signal, similar to Example 1 but with a different magnitude, i.e. $d(k) = 5$. The simulation results for this case are presented in **Figure 3**.

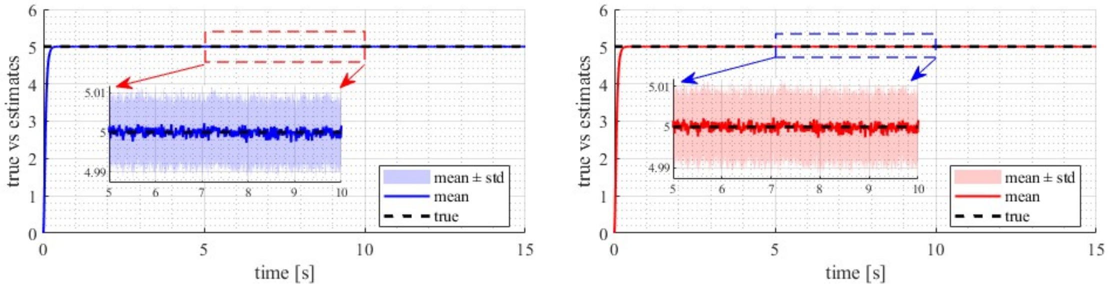

(a) Nominal KF ($\boldsymbol{Q} = 10^{20}\boldsymbol{I}_4$) (b) IPC-KF

Figure 3. Comparison of disturbance estimations for F-16 model with 100 random variables, Δ.

Figure 3 presents the disturbance estimation results for both the nominal KF and the IPC-KF. In **Figure 3(b)**, the diagonal elements of the $\bar{\mathbf{Q}}$ matrix are set to be twice those of the $\boldsymbol{Q}$ matrix. This adjustment is necessary because if the main diagonal values of $\bar{\mathbf{Q}}$ are equal to those of $\boldsymbol{Q}$, the disturbance estimation via IPC-KF tends to diverge. Therefore, $\bar{\mathbf{Q}}$ is defined as $\bar{\mathbf{Q}} = \mathrm{diag}\underbrace{(10^{40}, \cdots, 10^{40})}_{p+q} \otimes \boldsymbol{I}_{N+1}$, where the larger diagonal entries may be required due to the increased state dimension induced by the PCE. As shown in **Figures 3(a)** and **3(b)**, the estimated disturbances closely match the actual values across all parameter realizations for both the nominal KF and the IPC-KF, although further tuning of $\boldsymbol{Q}$ and $\bar{\mathbf{Q}}$ is still required. Furthermore, the selected uncertainty levels and covariance values are chosen to represent representative stress-test scenarios and are applied consistently across all estimators rather than being tuned for optimal performance.

3.3 Performance Metric Evaluation

To quantitatively assess the estimation performance of the IPC-KF and compare it with the nominal KF, we employ performance metrics suitable for stochastic systems with probabilistic parameters. In this evaluation, two metrics are used for both case studies, based on 100 realizations: the variance of the estimation results and the root-mean-square error (RMSE).

The variance indicates the estimator's sensitivity to parameter uncertainty and measurement noise; a smaller variance reflects a more stable and robust estimator. In addition, the average RMSE over all realizations provides a global measure of the expected estimation error, capturing the combined effects of bias and variability. These metrics are sufficient to determine whether the IPC-KF delivers comparable or improved estimation accuracy relative to the nominal KF, without requiring formal hypothesis testing, which is beyond the scope of this paper. The results obtained from these evaluation metrics are summarized in Table 1.

Table 1. Performance evaluation metrics for disturbance estimation using the nominal KF and IPC-KF, computed over 100 realizations for Examples 1 and 2

Examples	**Performance Metrics (mean)**	**Methods**	
		Nominal KF	**IPC-KF**
1	Variance	0.2133	0.2133
	RMSE	1.67**901**	1.67**892**
2	Variance	8.1915×10^{-5}	8.1915×10^{-5}
	RMSE	1.11971	1.11971

Table 1 summarizes the performance metrics used to compare the nominal KF and the IPC-KF over 100 realizations of the disturbance estimation results. The metrics show that both estimators achieve essentially identical performance in terms of the mean variance and RMSE across the same set of realizations. The mean variance in Example 2 is noticeably smaller than in Example 1, indicating that the estimators are more robust to parameter variations under measurement noise in this scenario. Although the overall performance of the two estimators is comparable, the IPC-KF yields a slightly lower RMSE than the nominal KF in Example 1 when using the same parameter settings. However, for Example 2, achieving performance comparable to the nominal KF requires tuning the IPC-KF with larger noise-covariance values. This highlights that the IPC-KF is more sensitive to covariance selection, and thus careful tuning of its parameters is essential.

3.4 Limitation and Further Investigation

The IPC-KF developed in this study is based on the Intrusive Spectral Projection (ISP) approach, where the system dynamics are expressed directly in terms of polynomial expansion coefficients. Although the Non-Intrusive Spectral Projection (NISP) method offers a dimensional advantage, it requires numerous model evaluations to construct the surrogate system, making it unsuitable for real-time Kalman filtering. Moreover, NISP does not naturally provide the closed-form system matrices required for the prediction and update steps of the filter. In contrast, the intrusive approach yields an explicit high-dimensional deterministic system that can be seamlessly integrated into the KF framework, including the extended-state formulation for disturbance estimation. While this approach increases the system dimensionality, it provides a clearer and more direct pathway for estimator design.

Based on the simulation results in Examples 1 and 2, the IPC-KF does not exhibit a pronounced performance improvement over the nominal KF under the considered scenarios. This outcome motivates further discussion on the conditions under which uncertainty-aware filtering may provide tangible benefits. In particular, for linear systems with moderate levels of parameter uncertainty, the nominal KF already operates close to optimality, which naturally limits the observable performance gains achievable by extensions such as the IPC-KF.

Nevertheless, the IPC-KF provides added value beyond pointwise estimation accuracy. Through the polynomial chaos representation, the proposed framework enables direct access to higher-order statistical information—such as the variance and confidence bounds of the estimated states and disturbances—without relying on repeated Monte Carlo simulations. This uncertainty-quantification capability offers interpretability regarding how parameter uncertainty propagates into the estimation process, which is not readily available in the nominal KF framework.

In this study, a constant disturbance is considered, as simulations indicate that the nominal KF implemented via an extended state observer for fixed parameters cannot accurately estimate time-varying disturbances (e.g., sinusoidal signals). Furthermore, the disturbance is modeled as a single augmented state variable to avoid unobservability issues in the resulting surrogate system.

To facilitate further research and validation, the MATLAB implementation of the IPC-KF method is publicly available at: https://github.com/heripurnawan/IPC-KF. A detailed sensitivity analysis with respect to uncertainty in Δ and variations in $\boldsymbol{Q}$ and $\boldsymbol{R}$ is beyond the scope of this paper and will be explored in future work, as it constitutes an independent and substantial research direction.

4. CONCLUSION

This paper investigated the performance of the IPC-KF for estimating unknown disturbances in systems with probabilistic parameters and measurement noise using two case studies: a spring–mass–damper system and an F-16 aircraft model. Through intrusive stochastic projection, the IPC-KF transforms the stochastic dynamics into a deterministic augmented system, enabling estimation under parameter uncertainty within a unified framework. The results show that the IPC-KF incorporates parameter-distribution information via polynomial chaos while producing disturbance estimates comparable to those of the nominal KF, indicating that for the considered uncertainty levels and configurations, estimation accuracy is not significantly altered. Nevertheless, the IPC-KF provides a structured way to represent and propagate parametric uncertainty, which may be advantageous in situations involving stronger uncertainty, nonlinear dynamics, or time-varying disturbances. In such settings, polynomial chaos offers richer statistical information beyond pointwise estimates. Future work will consider broader classes of systems, uncertainty levels, and operating conditions, as well as comparisons with alternative approaches such as DO-based estimators and non-intrusive polynomial chaos methods, which may help reduce computational complexity while preserving uncertainty-awareness.

ACKNOWLEDGEMENTS

This work was supported by DPPM KEMDIKTISAINTEK through the 2025 Research Early Career Lecturer (PDP) program under Contract No. 128/C3/DT.05.00/PL/2025 and derivative researcher contract No. 010/SP2II/PL/LITBANGPEMAS/2025. The authors would like to thank the anonymous reviewers for their valuable comments and suggestions, which have helped to improve the quality of this manuscript.

5. REFERENCES

[1] H. Yang, F. Deng, Y. He, D. Jiao, and Z. Han, "Robust nonlinear model predictive control for reference tracking of dynamic positioning ships based on nonlinear disturbance observer," *Ocean Eng.*, vol. 215, p. 107885, 2020, doi: 10.1016/j.oceaneng.2020.107885.

[2] S. Liu, L. Wang, and X. V. Wang, "Sensorless force estimation for industrial robots using disturbance observer and neural learning of friction approximation," *Robot. Comput. Integr. Manuf.*, vol. 71, p. 102168, 2021, doi: 10.1016/j.rcim.2021.102168.

[3] P. Ye, Y. Guan, S. Mao, P. Wang, and H. Zhu, "Contact Force Estimation for Robotic Manipulators based on Disturbance Kalman Filter," in *2023 IEEE International Conference on Robotics and Biomimetics (ROBIO)*, 2023, pp. 1–6. doi: 10.1109/ROBIO58561.2023.10354780.

[4] J. Fisher and R. Bhattacharya, "Linear quadratic regulation of systems with stochastic parameter uncertainties," *Automatica*, vol. 45, no. 12, pp. 2831–2841, 2009, doi: 10.1016/j.automatica.2009.10.001.

[5] E. Acar, G. Bayrak, Y. Jung, I. Lee, P. Ramu, and S. S. Ravichandran, "Modeling, analysis, and optimization under uncertainties: a review," *Struct. Multidiscip. Optim.*, vol. 64, no. 5, pp. 2909–2945, 2021, doi: 10.1007/s00158-021-03026-7.

[6] A. Herbut and W. Brzakala, "Polynomial chaos expansion vs. Monte Carlo simulation in a stochastic analysis of wave propagation," *Wave Motion*, vol. 130, p. 103390, 2024, doi: 10.1016/j.wavemoti.2024.103390.

[7] J. Son and Y. Du, "An efficient polynomial chaos expansion method for uncertainty quantification in dynamic systems," *Appl. Mech.*, vol. 2, no. 3, pp. 460–481, 2021, doi: 10.3390/applmech2030026.

[8] B. Enderle, B. Rauch, F. Grimm, G. Eckel, and M. Aigner, "Non-intrusive uncertainty quantification in the simulation of turbulent spray combustion using polynomial chaos expansion: A case study," *Combust. Flame*, vol. 213, pp. 26–38, 2020, doi: 10.1016/j.combustflame.2019.11.021.

[9] A. Koirala, T. Van Acker, R. D'hulst, and D. Van Hertem, "Uncertainty quantification in low voltage distribution grids: Comparing Monte Carlo and general polynomial chaos approaches," *Sustain. Energy, Grids Networks*, vol. 31, p. 100763, 2022, doi: 10.1016/j.segan.2022.100763.

[10] J. A. Paulson, S. Streif, R. Findeisen, R. D. Braatz, and A. Mesbah, "Fast stochastic model predictive control of end-to-end continuous pharmaceutical manufacturing," in *Computer Aided Chemical Engineering*, vol. 41, Elsevier, 2018, pp. 353–378. doi: 10.1016/B978-0-444-63963-9.00014-2.

[11] H. Purnawan, T. Asfihani, S. Kim, and S. Subchan, "Model Predictive Control Design under Stochastic Parametric Uncertainties Based on Polynomial Chaos Expansions for F-16 Aircraft," *J. Robot. Control*, vol. 5, no. 3, pp. 723–732, 2024, doi: 10.18196/jrc.v5i3.21366.

[12] H. Purnawan, T. Asfihani, S. Kim, and S. Subchan, "Stochastic model predictive control for flight path angle tracking of f-16 aircraft based on polynomial chaos," in *2024 International Seminar on Intelligent Technology and Its Applications (ISITIA)*, 2024, pp. 599–604. doi: 10.1109/ISITIA63062.2024.10668152.

[13] F. Zhang *et al.*, "Joint estimation of vehicle state and parameter based on maximum correntropy adaptive unscented Kalman filter," *Int. J. Automot. Technol.*, vol. 24, no. 6, pp. 1553–1566, 2023, doi: 10.1007/s12239-023-0125-3.

[14] R. Bhusal and K. Subbarao, "Generalized polynomial chaos-based ensemble Kalman filtering for orbit estimation," in *2021 American Control Conference (ACC)*, 2021, pp. 4290–4295. doi: 10.23919/ACC50511.2021.9482961.

[15] A. Kaldmäe and Ü. Kotta, "A brief tutorial overview of disturbance observers for nonlinear systems: application to flatness-based control," *Proc. Est. Acad. Sci.*, vol. 69, no. 1, pp. 57–73, 2020, doi: 10.3176/proc.2020.1.07.

[16] H. Purnawan, T. Asfihani, and S. Subchan, "Disturbance observer model predictive control with application to UAV pitch angle control," in *AIP Conference Proceedings*, 2022. doi: 10.1063/5.0116990.

[17] S. Subchan, L. R. Amalia, T. Asfihani, and H. Purnawan, "Reference Tracking of Quadrotor Using Modified Nonlinear Model Predictive Control Based on Nonlinear Disturbance Observer," in *International Conference on Mathematics: Pure, Applied and Computation*, 2023, pp. 87–104. doi: 10.1007/978-981-97-2136-8_8.

[18] B. A. Iza, Q. A. Fiddina, H. N. Fadhilah, D. K. Arif, and Mardlijah, "Automatic Guided Vehicle (AGV)

tracking model estimation with Ensemble Kalman Filter," in *AIP Conference Proceedings*, 2022. doi: 10.1063/5.0118817.

[19] H. Purnawan, "Desain Disturbance Observer-Based Stochastic Model Predictive Control Untuk Sistem Dengan Ketidakpastian Parameter Dan Gangguan," Institut Teknologi Sepuluh Nopember, 2024.

[20] K. Kumar, R. K. Tiwari, S. Bhaumik, and P. Date, "Polynomial chaos Kalman filter for target tracking applications," *IET Radar, Sonar \& Navig.*, vol. 17, no. 2, pp. 247–260, 2023, doi: 10.1049/rsn2.12338.

[21] L. Zhang, X. Liu, G. Zong, and W. Wang, "Kalman filter-based SMC for systems with noise and disturbances: applications to magnetic levitation system," *Int. J. Syst. Sci.*, pp. 1–13, 2025, doi: 10.1080/00207721.2025.2468364.

[22] X. Lin, W. Li, S. Li, J. Ye, C. Yao, and Z. He, "Combined adaptive robust Kalman filter algorithm," *Meas. Sci. Technol.*, vol. 32, no. 7, p. 75015, 2021, doi: 10.1088/1361-6501/abf57c.

[23] P. Listov, J. Schwarz, and C. N. Jones, "Stochastic optimal control for autonomous driving applications via polynomial chaos expansions," *Optim. Control Appl. Methods*, vol. 45, no. 1, pp. 3–28, 2024, doi: 10.1002/oca.3047.

[24] D. Sivaraman, S. Ongwattanakul, B. M. Pillai, and J. Suthakorn, "Adaptive polynomial Kalman filter for nonlinear state estimation in modified AR time series with fixed coefficients," *IET Control Theory \& Appl.*, vol. 18, no. 14, pp. 1806–1824, 2024, doi: 10.1049/cth2.12727.

[25] S. Kim, V. M. Deshpande, and R. Bhattacharya, "Robust Kalman Filtering with Probabilistic Uncertainty in System Parameters," *IEEE Control Syst. Lett.*, vol. 5, no. 1, pp. 295–300, 2021, doi: 10.1109/LCSYS.2020.3001490.

[26] N. Wiener, "The homogeneous chaos," *Am. J. Math.*, vol. 60, no. 4, pp. 897–936, 1938, doi: 10.2307/2371268.

[27] R. H. Cameron and W. T. Martin, "The orthogonal development of non-linear functionals in series of Fourier-Hermite functionals," *Ann. Math.*, pp. 385–392, 1947, doi: 10.2307/1969178.

[28] D. Xiu and G. E. Karniadakis, "The Wiener--Askey polynomial chaos for stochastic differential equations," *SIAM J. Sci. Comput.*, vol. 24, no. 2, pp. 619–644, 2002, doi: 10.1137/S1064827501387826.

[29] J. A. Paulson, A. Mesbah, S. Streif, R. Findeisen, and R. D. Braatz, "Fast stochastic model predictive control of high-dimensional systems," in *53rd IEEE Conference on decision and Control*, 2014, pp. 2802–2809. doi: 10.1109/CDC.2014.7039819.

[30] J. A. Paulson and A. Mesbah, "An efficient method for stochastic optimal control with joint chance constraints for nonlinear systems," *Int. J. Robust Nonlinear Control*, vol. 29, no. 15, pp. 5017–5037, 2019, doi: 10.1002/rnc.3999.

[31] B. Lu and F. Wu, "Probabilistic robust control design for an f-16 aircraft," in *AIAA Guidance, Navigation, and Control Conference and Exhibit*, 2005, p. 6080. doi: 10.2514/6.2005-6080.